

Complex apodized Lyot coronagraph for exoplanet imaging with partially obscured telescope apertures

John Trauger*, Dwight Moody, Brian Gordon
Jet Propulsion Laboratory, California Institute of Technology
4800 Oak Grove Drive, Pasadena, CA 91109 USA

ABSTRACT

We update the design, performance, and future prospects for the complex apodized Lyot coronagraph. We extend previous design work for off axis telescope with unobscured circular pupils, now to designs for high-contrast exoplanet imaging and spectroscopy with complicated pupil obscurations such as the WFIRST/AFTA telescope. Together with a pair of deformable mirrors for active wavefront control, the complex apodized Lyot coronagraph creates high contrast dark fields of view extending to within angular separations of $3 \lambda/D$ from the central star, over spectral bandwidths of 10% or more, and with throughput efficiencies greater than 35%.

Keywords: exoplanet, coronagraph, active optics

1. INTRODUCTION

Exoplanets ranging in size from Earth-like to Jovian, when imaged in reflected starlight, will be fainter than their parent stars by factors of 10^{-9} to 10^{-10} . For direct imaging in reflected starlight, the observatory must provide raw image contrast of 10^{-9} or better, which with post-processing of image data will extend detection sensitivities an order of magnitude fainter¹. We make reference to the ACCESS exoplanet mission concept study^{2,3} to place our laboratory objectives in the context of a representative, well-studied probe class mission concept.

An actively corrected space coronagraph forms a high contrast “dark field” where faint planets and orbiting dust/debris disks can be separated from the overwhelming glare of the central star, enabling the characterizations. Inner working angles of $2-3 \lambda_0/D$ are feasible with the Lyot coronagraph. The outer working angle is defined by the extent of the high contrast dark field, assumed here to be $23 \lambda_0/D$, corresponding to the highest spatial frequency controlled by a deformable mirror (DM) within the coronagraph with 48 actuators across the pupil diameter D . The dark field of view is characterized as a background of coherent speckles scattered from the central star into the dark field. High contrast is hardest to achieve at field angles closest to the target star. This work addresses the challenge of maintaining uniform high contrast across the dark field from the inner to outer working angles.

Our objectives are to demonstrate that the Lyot approach is capable of raw image contrast at the 10^{-9} level or better, and that its performance is stable and repeatable. This mirrors the approach for TPF-C Milestones #1 and #2^{4,5}, which respectively demonstrated monochromatic and broadband (10%) starlight suppression in the High Contrast Imaging Testbed (HCIT)⁶, but with a smaller inner working angle and broader spectral bandwidths. Here, spectral bandwidth is defined as the ratio $\delta\lambda/\lambda_0$, where $\delta\lambda$ is the full width at half maximum transmittance of the band-defining optical filter and λ_0 is the central wavelength. The inner and outer working angles (IWA and OWA) are defined in terms of the central wavelength λ_0 and the diameter D of the aperture stop on the deformable mirror (DM), which is the pupil-defining element of the laboratory coronagraph.

Laboratory experiments have validated our performance models, thereby establishing that the behavior is thoroughly understood. Our optical propagation models, based on the Fresnel approximation, incorporate the physical characteristics of the Lyot coronagraph elements, mirror surfaces, the deformable mirror, and the CCD imager. Since the underlying physics is not in question, the accuracy of our model predictions is essentially a test of the fidelity of our physical descriptions of the coronagraph elements. These models consistently predict laboratory contrast performance within ~15%, based on prior demonstrations in the HCIT, including TPF-C Milestones #1 and #2, and on more recent coronagraph demonstrations in the HCIT at up to 20% bandwidth.^{7,8,9}

So to summarize, our design objectives are as follows. (1) Raw contrast to be better than 10^{-9} at visible (450–950 nm) wavelengths. This is required to see exoplanet in reflected starlight, and can only be done from space. This contrast level is beyond the reach of large ground based telescopes, which are expected to achieve contrasts to 10^{-7} – 10^{-8} in the

coming decade. (2) Tolerance to telescope pointing jitter pointing and finite stellar diameters, both of order 1 milliarcsecond, while preserving high contrast performance. (3) Spectral bandwidth $\delta\lambda/\lambda_0$ greater than 10%, as will be required to capture scarce photons and enable color photometry and spectroscopy. (4) Inner and outer working angles: $3 \lambda/D$ or closer to the star to capture significant numbers of exoplanets, extending to $20 \lambda/D$ or more to cover exoplanet systems, debris disks, and enabling identification of background objects. (5) Coronagraph efficiency, defined in terms of throughput losses introduced by the coronagraph elements in addition to losses in telescope optics and detectors, to be better than 30%, again to capture scarce photons. (6) And to minimize instrument complexity, using a minimum number of critical elements and alignments, leading to a system with reduced cost and risk, greater overall efficiency, accurate optical models, and reliable performance predictions.

2. THE LYOT CORONAGRAPH APPROACH

The focal plane Lyot mask is composed of two thin film layers on a glass substrate, one metallic such as nickel, the second a dielectric such as magnesium fluoride. The metal layer is dominant in defining the attenuation profile, while the dielectric provides an additional degree of freedom to control the wavefront phase as well. The design algorithm includes the thickness profiles of the metal and dielectric layers as well as the actuator settings on a pair of deformable mirrors, which are all treated simultaneously as free parameters. I.e., our multilayer thin film interference code (which generates thickness profiles to match specified attenuation and phase profiles) is combined with our wavefront control optimization code (which finds the optimal deformable mirror settings for optical propagation in a realistic coronagraph). Our optical propagation code, written in Python, has been cross checked with the publicly-available PROPER code¹⁰ for prior hybrid Lyot designs, demonstrating agreement to within computer rounding errors. Starting with a band-limited¹¹ design for the real and imaginary parts of the complex occulter attenuation profile at the 550 nm central wavelength, the code generates physically realizable design adjustments against criteria that balance spectral bandwidth, contrast, inner working angle, and overall throughput.

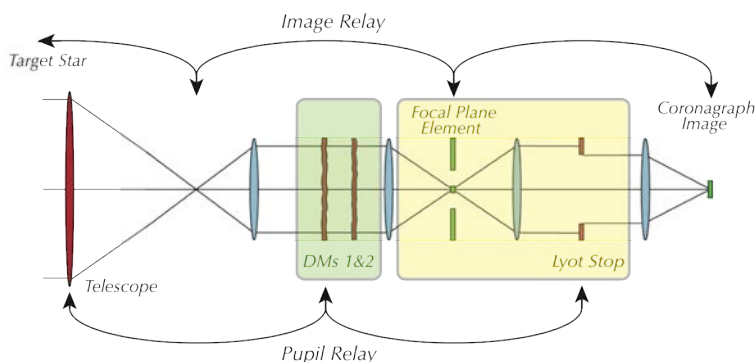


Figure 1. Sketch of the essential elements of the actively corrected Lyot coronagraph. Coronagraph elements are highlighted in yellow, wavefront control elements in green. Diagram unfolds the optical system and depicts powered elements as lenses for clarity. The coronagraph includes just two elements, a focal plane mask and a pupil stop. Amplitude and phase of the optical wavefront are manipulated with a sequential pair of deformable mirrors in the collimated beam upstream from the coronagraph.

The Lyot approach is among the simplest methods for high contrast coronagraphy, with a minimal number of critical optical elements between the star and coronagraph that are subject to super-tight optical tolerances. A minimum of optical elements favors lower cost and risk, higher throughput, and fewer critical optical alignments, and leads to a system with reduced cost and risk, greater overall efficiency, accurate optical models, and reliable performance predictions. For example, given a cassegrain telescope, one fold, one collimating mirror, two DMs, and a focusing mirror in the optical beam upstream of the Lyot focal plane mask, that number can be as small as seven. The optical layout requires no high-angle reflective elements, minimizing polarization effects internal to the coronagraph. Apodizers and/or polarizers are not required upstream of the focal plane occulter, and therefore no transmissive elements, which works to minimize the effects of dispersion and other chromatic complications. The critical apodization is captured on a small occulting mask, with one metal and one dielectric thin film layer on a glass substrate, which will be inherently stable and robust for flight. It is a conventional optical system, without optical distortions, which makes iterative wavefront sensing

and control straightforward. The simplicity of the optical system means that end-to-end optical propagation calculations (with the Fresnel approximation) and system optical tolerancing are relatively straightforward. Ultimately, simplicity tends to minimize the number of individual components, engineering interfaces, mutual alignments which can snowball in the buildup of assembly fixtures and metrology, alignment tolerances, failure modes and risk analysis, engineering subsystem coordination and reviews, subsystem integrations and tests – and these ultimately increase the cost, mass, schedule, and overall risk of the instrument implementation.

3. CIRCULAR LYOT DESIGN FOR THE IDEAL UNOBSCURED APERTURE

For comparison with the obscured apertures, we review an earlier investigation of high performance circular Lyot masks with inner working angles as small as $2.5 \lambda_0/D$ and spectral bandwidths greater than 18%.

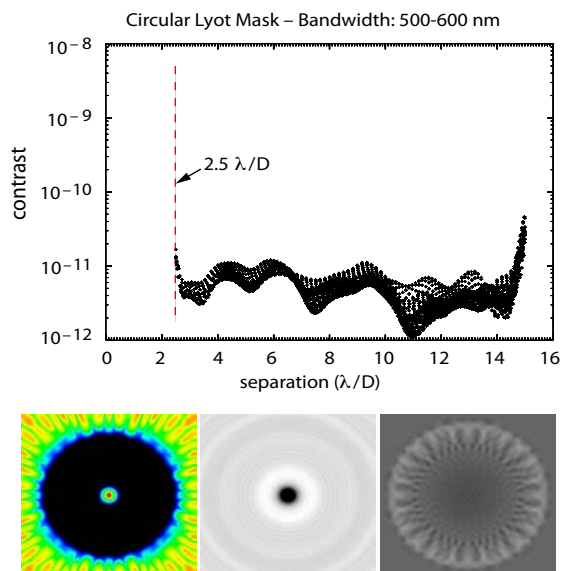


Figure 2. Predicted performance for a circular hybrid Lyot mask with a circular off-axis unobscured telescope aperture. Inner working angle is $2.5 \lambda_0/D$ with $\lambda_0 = 550 \text{ nm}$. The design optimization is carried out by varying thickness profiles of the metal and dielectric layers simultaneously with wavefront control by a single DM with a 48×48 array of actuators. Note that a full 360° dark field has been created with a single deformable mirror. Contrast in the 500–600 nm ($\delta\lambda/\lambda_0 = 18\%$) spectral band is 5.3×10^{-12} in both the inner $2.5\text{--}3.5 \lambda_0/D$ annulus and averaged across the entire dark field extending from radii of 2.5 to $15 \lambda_0/D$. The three images at bottom are: (left to right) the high contrast dark field displayed on a logarithmic contrast stretch from 10^{-11} to 10^{-7} , the intensity transmittance of the occulting mask on a linear scale from 0 to 1, and the DM figure pattern extending to $\pm 40 \text{ nm}$ of surface displacement.

Figure 2 shows an example designed for a $2.5 \lambda_0/D$ inner working angle and an 18% spectral bandwidth centered on $\lambda_0 = 550 \text{ nm}$. Dark field contrast is better than 1×10^{-11} over a high contrast dark field extending from 2.5 to $15 \lambda_0/D$, and over the 500–600 nm wavelength band. Note that this full dark field has been achieved with relatively small strokes of a single 48×48 actuator DM, by exploiting the ability of a DM to control the real and imaginary parts of the complex wavefront over half the controllable area (in this case, the central half of the controllable area, rather than the right or left half). Comparable results have been obtained for larger bandwidths up to 27% (475–625 nm) with predicted contrasts better than 1×10^{-9} over the entire dark field. The fabrication of these designs will be pursued as opportunities arise in the future.

4. LYOT MASKS OPTIMIZED FOR AN OBSCURED APERTURE

We discuss a preliminary, and very promising design approach specifically for the WFIRST/AFTA telescope, which we describe for these preliminary design exercise as a circular 2.4 meter primary mirror with a circular central obscuration and six linear features due to the struts of a hexapod mount for the secondary mirror. The optimization of the coronagraph system specifically includes as free parameters the thickness profiles of the focal plane occulting mask

(composed of one nickel and one MgF₂ layers), the shape and dimensions of the Lyot stop, and the surface figure settings on each of the two 48×48 actuator DMs. The procedure carries out a non-linear least squares optimization of a merit function, a weighted score based on our various performance objectives. The procedure is iterative, with small linear steps in the free parameters, basically the method of steepest descent, with parameter regularization to guide the convergence towards design objectives.

The design constraints include the following. The focal plane Lyot mask is circular symmetric with a peak attenuation no greater than an optical density of 4.5, for simplicity in the manufacturing. We assume an idealized 2.4 meter telescope with zero surface figure and alignment errors. Wavefront control is carried out with a pair of 48×48 DMs in series in a shared collimated beam. Inner working angle is $3 \lambda_0/D$ (142 milliarcsec with 2.4 meter telescope). Spectral bandwidth $\delta\lambda/\lambda_0 = 10\%$ spectral bandwidth centered at 550 nm. We assume that the source star has a 1 milliarcsec stellar diameter (roughly equal to the angular diameter of the sun at 10 pc) – i.e. we regard the star as a cluster of incoherent sources with the specified angular diameter in the sky.

The overall design figure of merit includes high contrast from the inner to outer working angles, high throughput, and minimal DM stoke. The optimization proceeds in steps, working from the solution for a simple unobscured telescope, then adding the complexity in successive steps. Parameters to allowed to move in an optimal sequence and in small linear steps. The telescope pupil representation progresses from an unobscured circular pupil, then adds central obscuration, then adds the struts. DM settings progress from single active DM in a pupil plan, then two DMs with simple rules, then two DMs with numerically optimized settings. The result, still a work in progress, is illustrated in the following figures.

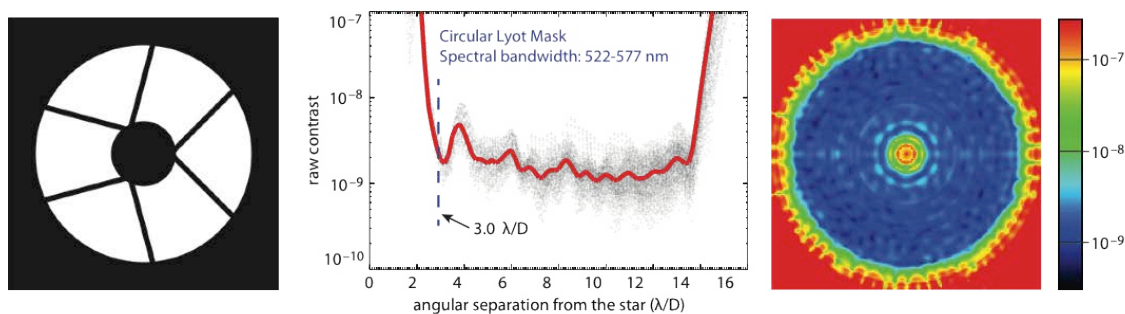


Figure 3. Preliminary hybrid Lyot coronagraph design adapted for an AFTA-like 2.4 meter telescope with central secondary mirror obscuration and six SM support struts as indicated at left. Design utilizes a circular metal-dielectric Lyot focal plane mask plus Lyot stop and wavefront control with a pair of 48×48 actuator DMs. Contrast has been optimized and computed here for a $3.0 \lambda_0/D$ inner working angle, $\delta\lambda/\lambda_0 = 10\%$ spectral bandwidth centered at $\lambda_0 = 550$ nm, and apparent stellar angular diameter of 1 milliarcsecond. Performance predictions are based on optical models that have been validated to the 2×10^{-10} contrast level in TDEM/H CIT demonstrations.⁹



Figure 4. The coronagraph elements. At left, the metal-dielectric focal plane mask controls both the real and imaginary parts of the star's point spread function. The intensity transmittance is illustrated here. At right, pupil plane (Lyot) mask has cutouts for the central obscuration and the six support struts.

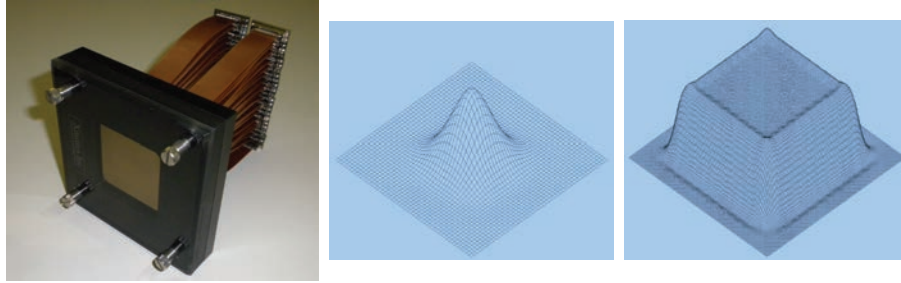


Figure 5. Wavefront control is modeled in terms of a pair of 48×48 actuator DMs, such as the Xinetics deformable mirror at right. At center, the measured surface figure influence function is illustrated at center, measured on a grid of points spaced by 0.1 mm, hence 100 sample points per actuator. The effect of the DM on wavefront phase is modeled by the simple superposition of these influence functions arrayed with a 1 mm pitch across the DM. An illustration of this linear superposition is seen at right, where an 11×11 subarray of the DM has been actuated to equal displacements, resulting in the expected table top and edge roll-off effects.

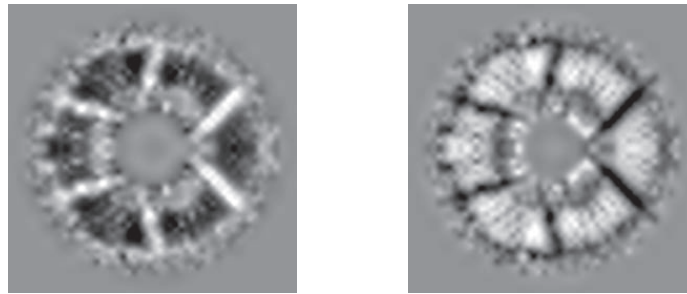


Figure 6. Shown here, the wavefront phase modulations introduced by the two 48×48 DMs with the foregoing occulting and Lyot masks. DM1 is at left, DM2 is at right. Surface displacements are $0.5 \mu\text{m}$ peak-to-valley. The design procedure evaluates a trade between shape of the Lyot stop in the previous figure, the DM settings, and overall throughput. These DM surface settings closely resemble each other in magnitude, but with the signs reversed, a result reminiscent of the ACAD strategy.¹² In fact, the pair of DMs can compensate entirely for the diffraction from the six struts using a circular symmetric Lyot stop (circular central obscuration without cutouts for the six struts), but would require an undesirably large $\sim 5 \mu\text{m}$ PV of DM surface displacement.

5. CONCLUSIONS

We have extended previous work with the metal-dielectric complex-apodized Lyot coronagraph design, this time for a telescope resembling the WFIRST/AFTA telescope, with a central secondary mirror obscuration and hexapod support struts. The preliminary design shown here indicates that these obscurations substantially reduce overall coronagraph performance in comparison with the ideal unobscured telescope, but that the Lyot coronagraph nevertheless provides contrast, inner working angle, spectral bandwidth, and overall throughput at the levels that will enable direct imaging and spectroscopy of exoplanet systems in reflected starlight at visible wavelengths. Ongoing work will further refine these designs, seeking better coronagraph performance and optimal tolerances to jitter and drift in the telescope optics, while accommodating the precise details of the AFTA telescope as such information becomes available. We have used our validated design procedure based on an agile software package that encompasses mask design, wavefront sensing and control, optical tolerancing and diagnostics, and realistic physical characteristics of the coronagraph and telescope. Our experience opens a new design path for extreme high contrast imaging with a wide variety of obscured telescopes, and we are optimistic that significant further advances will follow.

ACKNOWLEDGEMENTS

The research described in this paper was carried out at the Jet Propulsion Laboratory, California Institute of Technology, under a contract with the National Aeronautics and Space Administration.

REFERENCES

- [1] Trauger, J.T. and W.A. Traub, "A laboratory demonstration of the capability to image an Earth-like extrasolar planet," *Nature* **446**, 771 (2007).
- [2] Trauger, J. *et al.*, "ACCESS – A Concept Study for the Direct Imaging and Spectroscopy of Exoplanetary Systems," in *Pathways towards Habitable Planets, ASP Conf. Series* **430**, 375, 2010; and *Proc. SPIE* **7731**, 773128 (2010).
- [3] Trauger, J. *et al.*, "ACCESS – A space coronagraph concept for direct imaging and spectroscopy of exoplanetary systems," Public version of the Final Report to the NASA Astrophysics Strategic Concept Studies Program (2009).
- [4] Trauger, J. *et al.*, "TPF-C Milestone #1 Report," JPL Document D-35484 (2006).
- [5] Kern, B. *et al.*, "TPF-C Milestone #2 Report," JPL Document D-60951 (2008).
- [6] Trauger, J., A. Give'on, B. Gordon, B. Kern, A. Kuhnert, D. Moody, A. Niessner, F. Shi, D. Wilson, and C. Burrows, "Laboratory demonstrations of high-contrast imaging for space coronagraphy," *Proc. SPIE* **6693**, 66930X (2007).
- [7] Moody, D., B.L. Gordon, and J. Trauger, "Design and demonstration of hybrid Lyot coronagraph masks for improved spectral bandwidth and throughput," *Proc. SPIE* **7010**, 70103P (2008).
- [8] Trauger, J., D. Moody, B. Gordon, J. Krist, D. Mawet, "A hybrid Lyot coronagraph for the direct imaging and spectroscopy of exoplanet systems: recent results and prospects," *Proc. SPIE* **8151**, 81510G (2011).
- [9] Trauger, J., D. Moody, B. Gordon, J. Krist, D. Mawet, "Complex apodization Lyot coronagraphy for the direct imaging of exoplanet systems: design, fabrication, and laboratory demonstration," *Proc. SPIE* **8442**, 84424Q (2012).
- [10] Krist, J.E., "PROPER: an optical propagation library for IDL," *Proc. SPIE* **6675**, 66750P (2007).
- [11] Kuchner, M., and W. Traub, "A coronagraph with a band-limited mask for finding terrestrial planets," *Astrophys. J.* **570**, 900 (2002).
- [12] Pueyo, L. and C. Norman, "High contrast imaging with arbitrary apertures: active compensation of aperture discontinuities," *Astrophys. J.* **769**, 102 (2013).